Defence Science Journal, Vol. 69, No. 5, September 2019, pp. 474-480, DOI : 10.14429/dsj.69.14954

Development of Neural Network Based Adaptive Change Detection Technique for Land Terrain Monitoring with Satellite and Drone Images

Ankush Agarwal*, Sandeep Kumar, and Dharmendra Singh

Indian Institute of Technology, Roorkee - 247 667, India
**E-mail: ankushak28@gmail.com*

ABSTRACT

Role of satellite images is increasing in day-to-day life for both civil as well as defence applications. One of the major defence application while troop's movement is to know about the behaviour of the terrain in advance by which smooth transportation of the troops can be made possible. Therefore, it is important to identify the terrain in advance which is quite possible with the use of satellite images. However, to achieve accurate results, it is essential that the data used should be precise and quite reliable. To achieve this with a satellite image alone is a challenging task. Therefore, in this paper an attempt has been made to fuse the images obtained from drone and satellite, to achieve precise terrain information like bare land, dense vegetation and sparse vegetation. For this purpose, a test area nearby Roorkee, Uttarakhand, India has been selected, and drone and Sentinel-2 data have been taken for the same dates. A neural network based technique has been proposed to obtain precise terrain information from the Sentinel-2 image. A quantitative analysis was carried out to know the terrain information by using change detection. It is observed that the proposed technique has a good potential to identify precisely bare land, dense vegetation, and sparse vegetation which may be quite useful for defence as well as civilian application.

Keywords: Drone; Sentinel-2; Classification; Change detection; Time series; Terrain analysis

1. INTRODUCTION

Land-based terrain monitoring using high-resolution drone imagery in combination with multispectral satellite data has been widely used for various application including urban planning, agricultural crop characterisation, crop growth monitoring, forest ecosystem classification, terrain analysis, and various defence monitoring applications. Change detection in land use pattern is the major approach for analysing the human impact on the environmental changes that not only alter local landscape but also has an impact at distance from the source. Change detection has various applications in land use monitoring, the rate of deforestation analysis, coastal area change, urban extension, disaster effect, etc.

The temporal and spatial analysis procedures are useful in producing the statistical based scientific satellite data for understanding the land ecosystem dynamics and current terrain structure. For geographic resource decision support system, time series data provides detailed information for detecting and assessing change in land use and land cover dynamics[1]. This data is important for the defence evaluation of a geographical area. Terrain analysis gives the featured cover of land that helps in the formation of new defence models which maps for better strategic planning in mobility, based on standard defence procedures[2].

Change detection is the procedure for categorising the state evolution of an object or phenomenon perceived over time. This procedure used a high-resolution drone and satellite image for the change detection to identify the significant variables such as local texture and radiance regardless of viewing angle, illumination, soil moisture, and atmospheric condition.

The drone provides very high-resolution (VHR) images and accurate ground truth information, that can be used in the classification along with satellite images which result in improved accuracy and reliable classification. Various classification techniques such as K-means, ISODATA, Maximum Likelihood, Support Vector Machine (SVM), Neural Net etc., has been critically evaluated to classify remotely sensed data by using high-resolution drone imagery[3]. The application of artificial/fuzzy neural network on satellite data is used for the quality evaluation of regional eco-environment[4,5,6].

A deep-learning approach for the analysis of change detection in targets is carried out with the satellite time series data[7]. Change in area of snow cover can be estimated by the information generated with satellite imagery and ground-based measurements[8]. For accessing the performance of the neural network and calculate the effect of various parameters on classification for the change detection is carried out on IRS-1B LISS-II image[9].

These methods can be applied to various defence applications such as logistical planning at various terrain area and identification of the suitable area for movement, identification of enemy troop concentration at some specified region. A comparative study for target detection using hyperspectral images have a variety of application in both defence and

Received : 01 December 2018, Revised : 05 March 2019
Accepted : 20 April 2019, Online published : 17 September 2019

civilian[10]. In a comparison of the statistical approaches, new technology such as synthetic aperture radar (SAR) data and neural network is used for the target detection[11]. The work suggests neural networks and multisource data integration have great potential for analysing and interpreting targets. The multiresolution mapping and informative path planning help in UAV based terrain monitoring[12]. Use of aerial images acquired by UAV for object recognition based on convolution neural network is beneficial for civil and defence purposes[13].

Dense vegetation and sparse vegetation cannot be classified using google earth imagery because it is difficult to identify in the image. Generally, researchers are using google earth imagery for obtaining ground control points (GCPs). There is also a possibility to get sparse inside the field and it is difficult to move in for recording global positioning system (GPS) of each such locations. Therefore, this type of sparse and dense vegetation data can be obtained and segregated with drone data at a very high precision level.

The main motive of this paper is to classify bare land, dense vegetation and sparse vegetation with the Sentinel-2 satellite data. Monitoring of considered classes is useful in various applications like for planning troops moment in defence, terrain actual scenario, precision agriculture etc. Till now very less work is reported which deals with these type of classes. Therefore in this paper, a neural network based technique has been proposed to classify and monitor change in these classes.

The proposed technique is adaptive in a manner that a network is trained by considering the different conditions of the considered classes which reflects a quite good range of variation in considered classes.

There are numerous approaches to detect environmental/ land cover changes among which machine learning has been one popular approach as it provides better efficiency and ease in automation. Supplementary information from drones is widely used nowadays in land cover monitoring. The challenge here is a need for drone imagery to provide the precise level of terrain information so that neural network can be trained effectively. Therefore the objective of this research is to detect the change in pixel class, which may help the defence and others to know about the terrain behaviour at the precise level with the use of satellite images.

2. STUDY AREA AND DATA DESCRIPTION

2.1 Study Area

An area nearby Roorkee has been selected for study, which is an agricultural field located in the Uttarakhand state, the northern part of India. The field is bounded by 29.92840, 29.93264 N and 77.96278, 77.96610 E. The agriculture field consists of three main classes named as bare land, dense vegetation and sparse vegetation, whose class ID's (C_ID) are BL, DV, and SV respectively. These class IDs will be used as nomenclature in the further sections.

2.2 Data Description

2.2.1 Sentinel-2 Data

Sentinel-2 provides an optical high-resolution data to the registered users on the Copernicus Open Access Hub portal. It has 13 spectral bands with global coverage having a temporal period of 5 day with two sensors and 10 day with a single sensor named as S2A and S2B. The bands have different spatial resolutions of 10 m, 20 m, and 60 m[14]. Bands 8, 4, 3, and 2 that respectively represent NIR, Red, Green, and Blue channels have been used for the considered study. The map projection of the received data is in UTM WGS-84 N 44 zone. The data of Sep 12, 2017, Oct 07, 2017, Nov 16, 2017, and Dec 21, 2017, is acquired, whose date IDs (D_ID) are D1, D2, D3, and D4 respectively. These date IDs will be used as nomenclature in the further sections.

2.2.2 Drone Data

The drone with 4K resolution RGB camera is used and it has a GPS unit attached[15]. Consecutive images with a forward and cross overlap of 70 per cent are captured at the height of 100 m above the ground level. The images were stitched and geo-registered. The map projection of the stitched image is in UTM WGS-84 N 43 zone having a ground sampling distance of 0.05 m. Images from the drone are captured on the same dates as of Sentinel-2 acquisition dates over the study area.

3. METHODOLOGY

The workflow of the proposed methodology is carried in two different parts as shown in Fig. 1. In the first part, Sentinel-2 data is processed and in the second drone data is processed whose step-wise procedure is as shown in Fig. 1. The explanation of each step is given in the subsections.

3.1 Data Acquisition

3.1.1 Sentinel-2

Data is acquired from the ESA data pool for the four dates having D_ID: D1, D2, D3, and D4. The data is available at free of cost for the registered users and is open source.

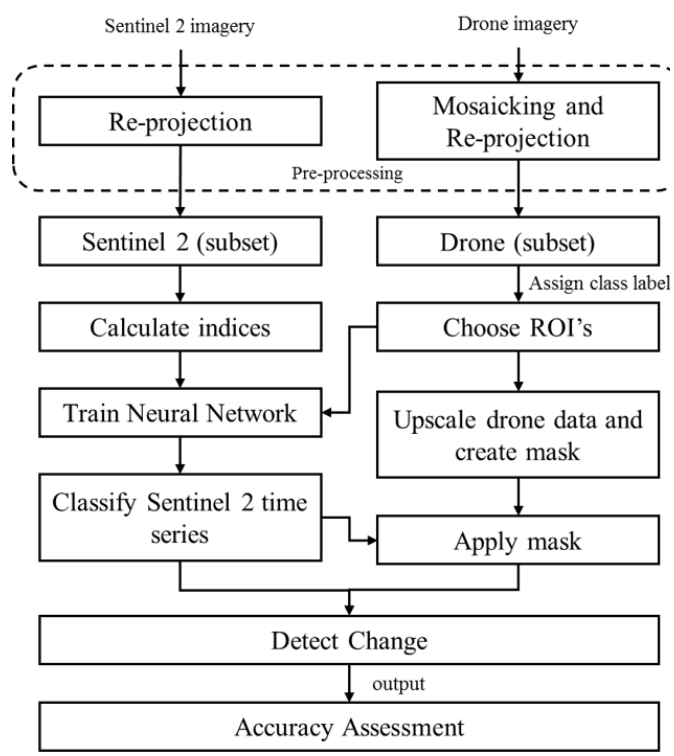

Figure 1. The workflow of the task.

3.1.2 Drone

Flight of Sentinel-2 was tracked and the drone was flown on the same dates over the study area to acquire the data. Drone data has various challenges such as ortho-rectification, calculation of ground sample distance etc. which were taken care at the time of flight. Once the still images are obtained, they are mosaicked to form a single image.

3.2 Data Pre-processing

3.2.1 Sentinel-2

Sentinel-2 imagery needs to be atmospherically corrected before using it, which can be done with the help of Sen2Cor tool provided by ESA. It is a level-2 processor which can be used to correct the effect of top-of-atmosphere (TOA) and delivers a Level-2A bottom-of-atmosphere (BOA) product[16]. The obtained BOA product has to be multiplied with a factor of 0.0001 to obtain corrected surface reflectance value. Then Sentinel-2 data is re-projected to Geographic Lat/Long.

3.2.2 Drone Images

For further processing, the mosaicked drone image is re-projected to Geographic Lat/Long.

3.3 Subset

A subset of both drone and Sentinel-2 imagery has been taken, having the same area and bounding coordinates which have a pixel count of 48 x 33 and 9600 x 6600, respectively. The re-projected subset images are as shown in Fig. 2.

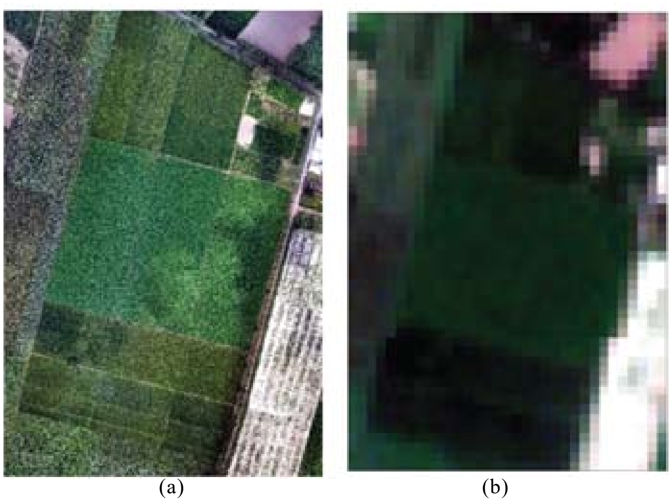

Figure 2. RGB imagery of D_ID: D1 (a) drone and (b) Sentinel-2 image.

3.4 Indices Calculation and Selection of ROI’s

3.4.1 Sentinel-2

Although numerous vegetation indices are available, three indices that are having unique significance related to vegetation have been used here. Normalised difference vegetation index (NDVI) is used to determine the density of greenness, modified soil adjusted vegetation index (MSAVI) determines the density of greenness by reducing the soil background influences and ratio vegetation index (RVI) estimates the green biomass. These indices are calculated (from Eqns. 1-3) and stacked date-wise. The purpose of choosing these indices is to identify the classes on the basis of a set of values rather than ground points.

$$NDVI = \frac{\rho_{NIR} - \rho_R}{\rho_{NIR} + \rho_R} \quad (1)$$

$$MSAVI = \frac{\rho_{NIR} - \rho_R}{\rho_{NIR} + \rho_R + L} * (1 + L) \quad (2)$$

$$RVI = \frac{\rho_R}{\rho_{NIR}} \quad (3)$$

where,

ρ_{NIR} *Near Infrared band*

ρ_R *Red band*

L 0.5

3.4.2 Drone Images

Drone imagery is having very high resolution and helps in choosing region of interest (ROI) of each class. The chosen ROI index location is then used to extract the indices value for each class which will be used in the training dataset.

3.5 Network Training

A neural network is designed to train the indices values with the chosen ROI of three classes obtained from Sentinel-2 reference image (D_ID: D1). This network has three input nodes, ten hidden layer neurons and three output nodes. At input nodes, the considered indices values are provided for training, which results in three output classes. The architecture of the considered neural network is as shown in Fig. 3.

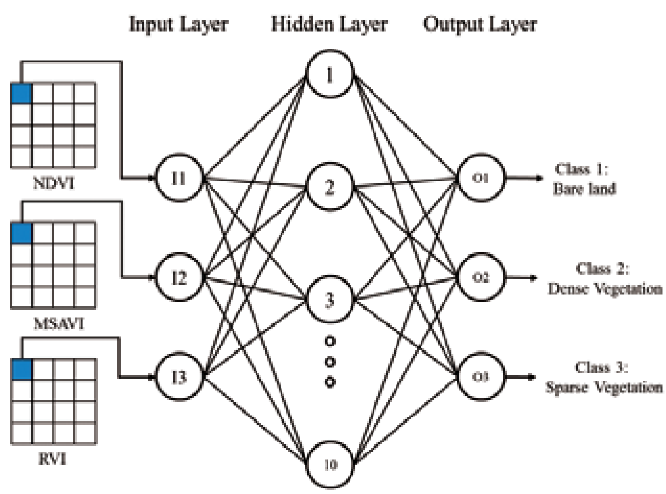

Figure 3. Neural network architecture.

3.6 Classification

The considered indices images were stacked for each date and passed to the trained network. The network now uses its training sets to classify the image and assigns a class label (C_ID: BL, DV, SV) to each pixel. The classification results are as shown in column (3) of Fig. 4 whereas column (1) and (2) displays drone and Sentinel-2 images.

As depicted in Fig. 4, pixel labels have changed over time, whose pixel count is as shown in Table 1.

3.7 Upscale of Drone Data

The spatial resolution of drone and Sentinel-2 are 0.05 m and 10 m respectively, therefore, a grid of 200x200 pixels is

Table 1. Pixel count with positive, negative and no-change deviation with the reference classified image (D_ID: D1)

C_ID \ D_ID	D1	D2	D3	D4
BL	262	708 +ve 446	1287 +ve 579	1345 +ve 58
DV	1054	488 -ve 566	0 -ve 488	0 no-change
SV	268	388 +ve 120	297 -ve 91	239 -ve 58

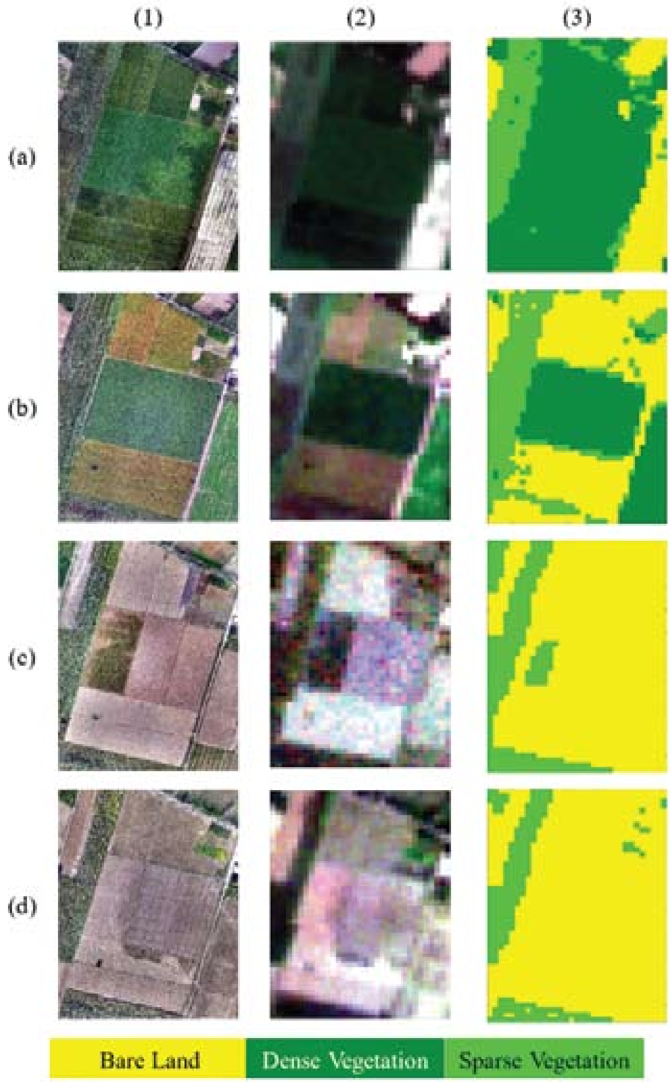

Figure 4. Drone, Sentinel-2 and classified Sentinel-2 image are shown in marked column 1-3 respectively. D_ID in row (a) D1, (b) D2, (c) D3 and (d) D4.

overlaid on the drone image to make it Sentinel-2 equivalent. A class label is assigned to every pixel of a drone image, then it is up-scaled, which is further used in generating the masks of three classes (C_ID: BL, DV, and SV) for testing the performance. The gridded, class labelled and the up-scaled classified drone image is as shown in Fig. 5.

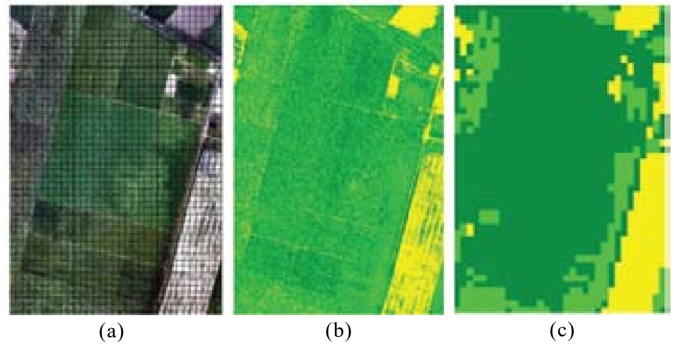

Figure 5. Drone imagery (a) Overlaid grid, (b) class labelled, and (c) up-scaled class labelled

3.8 Mask Generation

Masks for the three considered classes for the considered dates are generated from the up-scaled drone imagery. The white patch in the mask creation reveals the presence of desired class and black reveals the presence of another class. Pixel count of each class in the masks for each date is as shown in Table 2.

Table 2. Pixel count of each class in masks for each date

C_ID \ D_ID	D1	D2	D3	D4
BL	217	781	1169	1410
DV	1120	574	0	0
SV	247	229	415	174

3.9 Mask Overlay

The generated masks are applied to the classified Sentinel-2 images (sec. 3.6) of each date to detect the change in class label. Rows (a) - (d) of Fig. 6 shows the masking results of different dates and column (1) - (3) represents various classes. Yellow represents bare land, dark green represents dense vegetation, and light green represents sparse vegetation whereas red indicates false positive (which means presence in mask but classified as another class), blue indicates false negative (which means not in mask and on the other hand classified as a class member), and black indicates true negative (absence of class).

3.10 Change Detection and Accuracy Assessment

The change in class labels in the classified images is computed which further undergoes critical analysis over time.

4. RESULTS AND DISCUSSION

4.1 Study of Changes in Class Label

The occurrence of changes in the class label for each pixel of classified Sentinel-2 and drone image is calculated over the time using their respective reference image dated (D_ID: D1) as shown in Table 3(a) and 3(b), respectively. The pseudo code for the same is given below Count_Change_In_Label().

Actual pixels count of each class label for different dates is obtained using generated masks (as shown in Table 1). These masks were applied to the classified Sentinel-2 image and changes in pixel count is calculated (as shown in Fig. 6).

Mask results can be interpreted in terms of correctly classified, false positive, false negative and no-change pixel count as shown in Table 4.

```
Count_Change_In_Label(reference_image, input_image)
Declaration:
(i, j): indexes
cxy : counters where x,y: (1, 2, 3)
BL, DV, SV: class labels (C_ID)
Input:
ref ← reference_image
inp ← input_image
Begin:
for each pixel of inp
    if ref(i,j) = BL and inp(i,j) = BL
        c11 = c11 + 1;
    elseif ref(i,j) = BL and inp(i,j) = DV
        c12 = c12 + 1;
    elseif ref(i,j) = BL and inp(i,j) = SV
        c13 = c13 + 1;
    elseif ref(i,j) = DV and inp(i,j) = BL
        c21 = c21 + 1;
    elseif ref(i,j) = DV and inp(i,j) = DV
        c22 = c22 + 1;
    elseif ref(i,j) = DV and inp(i,j) = SV
        c23 = c23 + 1;
    elseif ref(i,j) = SV and inp(i,j) = BL
        c31 = c31 + 1;
    elseif ref(i,j) = SV and inp(i,j) = DV
        c32 = c32 + 1;
    elseif ref(i,j) = SV and inp(i,j) = SV
        c33 = c33 + 1;
end for
End
```

Table 3. Changes observed in the class label of each pixel of classified (a) Sentinel-2 (b) drone images

(a)

C_ID \ D_ID	D1 → D2	D1 → D3	D1 → D4
BL → BL	109	245	256
BL → DV	134	0	0
BL → SV	19	17	6
DV → BL	546	915	962
DV → DV	347	0	0
DV → SV	161	139	92
SV → BL	53	127	127
SV → DV	7	0	0
SV → SV	208	141	141

(b)

C_ID \ D_ID	D1 → D2	D1 → D3	D1 → D4
BL → BL	104	172	207
BL → DV	112	0	0
BL → SV	1	45	10
DV → BL	571	839	1005
DV → DV	403	0	0
DV → SV	146	281	115
SV → BL	106	158	198
SV → DV	59	0	0
SV → SV	82	89	49

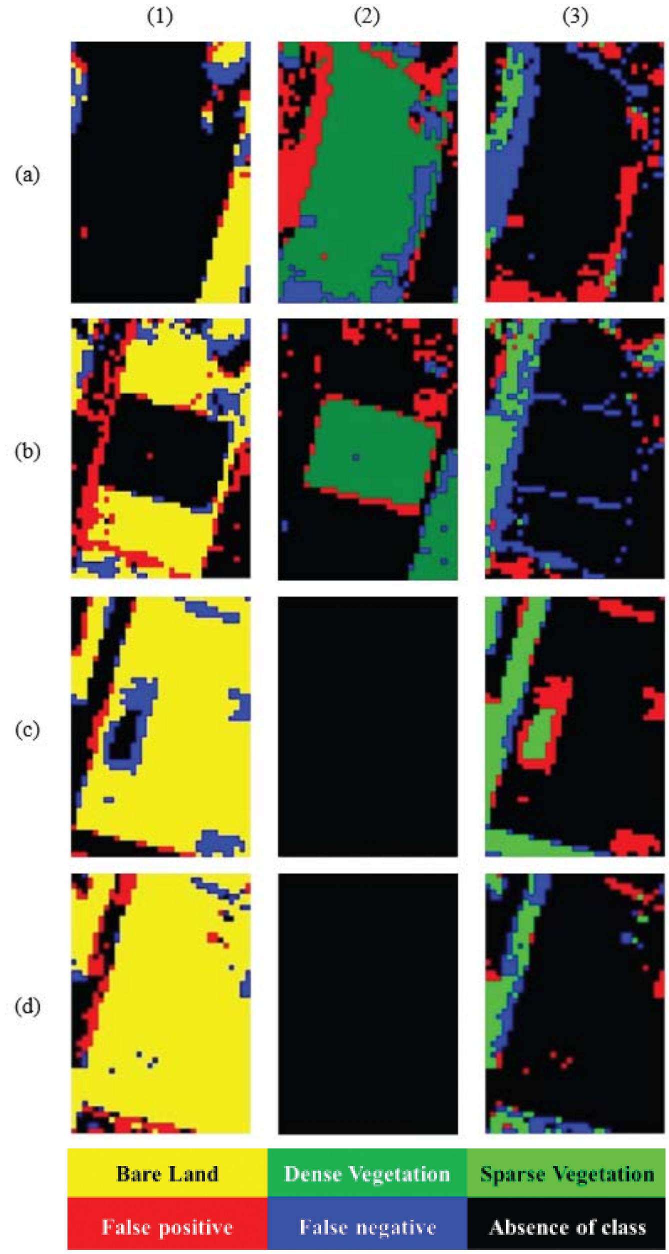

Figure 6. Mask results of three classes applied on the classified Sentinel-2 image is in column 1-3 of C_ID: BL, DV, and SV respectively. D_ID in rows (a) D1, (b) D2, (c) D3, and (d) D4.

Table 4. Pixel count of change/no-change pixel of each class in Sentinel-2 data

C_ID \ D_ID	D1	D2	D3	D4
BL → BL	182	579	1122	1297
BL → DV	22	27	0	0
BL → SV	13	175	47	113
DV → BL	57	68	0	0
DV → DV	873	453	0	0
DV → SV	190	53	0	0
SV → BL	23	61	165	48
SV →DV	159	8	0	0
SV → SV	65	160	250	126

4.2 Accuracy Assessment

Class wise accuracy along with an overall accuracy (in %) is as shown in Table 5 which reports a good overall accuracy. In the context of class-wise accuracy, it is found that the contribution of sparse vegetation is comparatively less whereas bare land and dense vegetation classes are classified with high precision. It is also clear from the table that the overall accuracy has good agreement with results.

Table 5. Class-wise accuracy with overall accuracy for each date

C_ID \ D_ID	D1	D2	D3	D4
BL	83.87	74.13	95.97	91.98
DV	77.94	78.91	100	100
SV	26.31	69.86	60.24	72.41
Overall Accuracy	70.7	75.25	86.61	89.83

Considering the scenario, where we are comparing class accuracies in one vs other classes, then we even get better results which are shown in Table 6.

Table 6. Confusion matrix

C_ID \ D_ID	D1	D2	D3	D4
BL	92.73	79.10	86.61	89.83
DV	72.97	90.15	100	100
SV	75.69	81.25	86.61	89.83

5. CONCLUSIONS

Drone data has been successfully used as supplementary information with satellite data, to detect the change in terrain behaviour. Drone data is used here to train the neural network, whose outcome can be used on future datasets without further training. Terrain information can be calculated precisely which may be beneficial for defence as well as civilian purpose. Quantitative analysis has been performed in this study, which can be used in the future for various applications like in defence for planning troops movement, terrain actual scenario, precision agriculture, etc.

REFERENCES

1. Adedeji, O. H.; Tope-Ajayi, O. O. & Abegunde, O. L. assessing and predicting changes in the status of Gambari Forest Reserve, Nigeria using remote sensing and GIS techniques. *J. Geogr. Inf. Syst.* 2015, **7**, 301–318. doi: 10.4236/jgis.2015.73024.
2. Hudson, R.D. & Hudson, J. W. The military applications of remote sensing by infrared. *Proc. IEEE,* 1975, **63**, 104-128. doi: 10.1109/PROC.1975.9711.
3. Agarwal, A.; Singh, A.K.; Kumar, S. & Singh, D. Critical analysis of classification techniques for precision agriculture monitoring using satellite and drone. *In* IEEE 13th International Conference on Industrial and Information Systems (ICIIS), 2018, pp. 83–88. doi: 10.1109/ICIINFS.2018.8721422.
4. Shi, Z. & Li, H. Application of artificial neural network approach and remotely sensed imagery for regional eco-environmental quality evaluation. *Environ. Monit. Assess.,* 2007, **128**, 217–229. doi: 10.1007/s10661-006-9307-5.
5. Nemmour, H. & Chibani, Y. Fuzzy neural network architecture for change detection in remotely sensed imagery. *Int. J. Remote Sens.*, 2006, **27**, 705–717. doi: 10.1080/ 01431160500275648.
6. Gopal, S. & Woodcock, C. Remote sensing of forest change using artificial neural networks. *IEEE Trans. Geosci. Remote Sens.*, 1996, **34**, 398–404. doi: 10.1109/36.485117.
7. Ignatiev, V.; Trekin, A.; Lobachev, V.; Potapov, G. & Burnaev, E. Targeted change detection in remote sensing images. 2018, 1–10. arXiv:1803.05482 [cs.CV].
8. Negi, H. S.; Mishra, V. D. & Mathur, P. Change detection study for snow covered mountains using remote sensing and ground based measurements. *J. Indian Soc. Remote Sens.,* 2005*,* **33**, 245–251. doi: 10.1007/ BF02990042.
9. Tiwari, K. C. Neural network parameters affecting image classification. *Def. Sci. J.,* 2002, **51**, 263–278. doi: 10.14429/dsj.51.2237.
10. Arora, M.K.; Bansal, S.; Khare, S. & Chauhan, K. Comparative assessment of some target detection algorithms for hyperspectral images. *Def. Sci. J.,* 2013, **63**, 53–62. doi: 10.14429/dsj.63.3764.
11. Chaudhuri, B. B. & Parui, S. K. Target Detection: Remote Sensing Techniques for Defence Applications. *Def. Sci. J.,* 2013*,* **45**, 285–291. doi: 10.14429/dsj.45.4135.
12. Popovic, M. *et al.* Multiresolution mapping and informative path planning for UAV-based terrain monitoring. *IEEE Int. Conf. Intell. Robots Syst.* 2017, 1382–1388. doi: 10.1109/IROS.2017 .8202317.
13. Radovic, M.; Adarkwa, O. & Wang, Q. Object Recognition in Aerial Images Using Convolutional Neural Networks. *J. Imaging,* 2017, **3**, 21. doi: 10.3390/jimaging3020021.
14. Sentinel data access overview - Sentinel online. Available at: https://sentinel.esa.int/ web/sentinel/sentinel-data-access; jsessionid=D 6A26107B9CDFA76CA93E2 DD1B3143F2.jv m2. (Accessed on 28 July 2018).
15. Phantom 3 Professional - Let your creativity fly with a 4K camera in the sky. - DJI. *DJI Official* Available at: https://www.dji.com/ phantom-3-pro. (Accessed on 28 July 2018).
16. Sen2Cor | STEP. Available at: http://step.esa. int/main/ third-party-plugins-2/sen2cor/. (Accessed on 28 July 2018).

ACKNOWLEDGEMENTS

The author would like to extend appreciation to all the lab members especially Arun Kumar Singh and Ekta Panwar who have always inspired and supported in the work. Also, the author would like to express thanks to RailTel Corporation of India Ltd., Delhi for sponsoring this work.

CONTRIBUTORS

Mr Ankush Agarwal received his BTech in Information Technology from Uttar Pradesh Technical University, Lucknow, India in 2007, MTech in Computer Science and Engineering from Indian Institute of Technology Roorkee, Roorkee, Uttarakhand, India in 2010 and is currently pursuing PhD in the Department of Computer Science and Engineering at Indian Institute of Technology Roorkee, Roorkee, Uttarakhand, India since July 2015. His main research interest includes the Internet of Things, Drone applications, agriculture monitoring, cloud computing and processing and Satellite image processing and analysis.
Contribution in the current study, he is the main contributor to this study. He conceived the idea of the current study and implemented the proposed algorithm.

Dr Sandeep Kumar is currently working as an Associate Professor in the Department of Computer Science and Engineering, Indian Institute of Technology Roorkee, India. He has published more than forty-five research paper in international/ national journals and conferences and has also written book/book-chapters with Springer (USA) and has filed two patent. He is currently handling multiple national and international research/consultancy projects. He has received NSF/TCPP early adopter award-2014, 2015, ITS Travel Award 2011 and 2013 and others. His name has also been enlisted in major directories such as Marquis Whos Who, IBC, and others. His areas of interest include Semantic Web, Web Services, and Software Engineering.
Contribution in the current study, he has supervised in the analysis of the data and its use for classification.

Dr Dharmendra Singh received the PhD in Electronics Engineering from IIT (BHU) Varanasi, India. He has 24 year of experience in teaching and research. He is currently a Professor with the Department of Electronics and Communication Engineering, IIT Roorkee, India, and a Head of the Department of Computer Science and Engineering, IIT Roorkee. His research interests include microwave remote sensing, polarimetry, interferometry, numerical modelling, data fusion, machine learning, computer vision, through-wall imaging and stealth technology.
Contribution in the current study he has framed the flow of study and supervised all the activities of the current research work.